QUANTITATIVE 3-D ELEMENTAL MAPPING BY LA-ICP-MS OF BASALTIC CLAST FROM THE HANFORD 300 AREA, WASHINGTON, USA

Sheng Peng, Qinhong Hu*, Robert P. Ewing, Chongxuan Liu, and John M. Zachara

SUPPORTING INFORMATION

Contents

1. Instrumentation and operating conditions

A UP-213 laser ablation system (New Wave, Freemont, CA), interfaced with a PerkinElmer/SCIEX ELAN DRC II (Sheldon, CT) ICP-MS system, was used to characterize the elemental distribution in the basaltic clast sample. The liquid standards of 2 µg/L ^{6}Li, ^{45}Sc, ^{115}In, and ^{209}Bi were continuously introduced to monitor the ICP-MS stability and provide a basis for time-drift correction. During data acquisition, signal intensities (counts per second, CPS) were recorded for the contaminant elements of primary interest (^{238}U, ^{63}Cu, and ^{27}Al), other possible contaminants with lesser (or unknown) released amounts (^{51}V, ^{58}Ni, ^{137}Ba, and ^{232}Th), and several other elements intrinsic to the basalt with a range of atomic mass (e.g., ^{23}Na, ^{24}Mg, ^{29}Si, ^{39}K, ^{44}Ca, ^{54}Fe, ^{55}Mn, ^{85}Rb, ^{88}Sr, and ^{90}Zr). Please see Table S1 for more concrete operation conditions.

During a 7-second pause before laser firing, the measured signal intensity was used to determine the instrument background for each element. After laser firing, when the ablated sample reached the detector, there was a sharp rise in signal intensity, followed by a gradual return to background levels within a minute. After subtracting the background, the integrated signal intensity was obtained by adding all signals from this transient analysis. Differences in the integrated signal intensity of the elements reflect their differences in abundance/concentration within the ablated volume (1).

(1) Hu, Q.; Kneafsey, T.J.; Wang, J.S.Y.; Tomutsa, L.; Roberts, J.J. Characterizing unsaturated diffusion in porous tuff gravels. *Vadose Zone J*. **2004**, *3*, 1425–1438.

Table S1. Operation condition for LA-ICP-MS.

Laser ablation	
Laser system	New Wave UP213; Tempest Nd:YAG
Wavelength	213 nm
Output power (mJ)	2.8-3.0
Ablation chamber	New Wave SuperCell
Pulse duration (ns)	3-5
Spot size (µm)	100
Repetition rate (Hz)	20
Pre-ablation time (s)	6-10
ICP–MS	
Spectrometer	PerkinElmer Elan DRC II
Forward power (W)	1300
Argon flow rate	
Nebulizer Ar gas (L/min)	0.60
LA carrier He gas (L/min)	0.60
Auxiliary gas (L/min)	0.95
Cooling gas (L/min)	14.0
Spray chamber	cyclonic
Nebulizer	Meinhard® type A
Sample and skimmer cones	Platinum
Data acquisition mode	Peak jumping
Dwell time per peak (ms)	2 (Al, Si, and K), 5 (Na, Mg), 20 (all others)
Acquisition duration (s)	30-60 (dependent on the numbers of laser pulses)

Table S2. Eight major composition percentages for 13 rocks.

ID	rock	data source	major composition percentage									sum percentage
			Si	Al	Fe(II)	Fe(III)	Mg	Ca	Na	K	Mn	
1	basalt, Columbia River, Oregon, BCR-2	USGS Certificate of Analysis	25.3	7.1	0.0	9.7	2.2	5.1	2.3	1.5	0.0	53.2
2	Costa Rica basalt	microprobe data from PSU	25.3	9.2	5.2	0.0	1.8	6.4	2.0	1.1	0.1	51.2
3	grimsel granodiorite	LTD progress Meeting; May 2007	31.6	8.3	2.6	0.0	0.4	1.5	3.3	3.2	0.1	50.9
4	stripa granite	Introduction to the hydrogeochemical investigations within the International Stripa Project; Nordstrom et al., GCA, 53:1717-1726	35.9	7.4	0.0	0.9	0.2	0.5	3.0	3.8	0.0	51.8
5	Andesite AGV-2	USGS Certificate of Analysis	27.7	8.9	0.0	4.7	1.1	3.7	3.1	2.4	0.0	51.6
6	Dunite DTS-2	USGS Certificate of Analysis	18.4	0.2	0.0	5.4	29.8	0.1	0.0	0.0	0.0	54.0
7	granite G-2	USGS Certificate of Analysis	32.3	8.1	1.1	0.7	0.5	1.4	3.0	3.7	0.0	51.0
8	granodiorite GSP-2	USGS Certificate of Analysis	31.1	7.9	0.0	3.4	0.6	1.5	2.1	4.5	0.0	51.1
9	quartz latite QLO-1	USGS Certificate of Analysis	30.7	8.6	2.3	0.7	0.6	2.3	3.1	3.0	0.0	51.2
10	rhyolite RGM-1	USGS Certificate of Analysis	34.3	7.3	1.0	0.3	0.2	0.8	3.0	3.6	0.0	50.5
11	shale SGR-1	USGS Certificate of Analysis	27.7	8.9	0.0	4.7	1.1	3.7	3.1	2.4	0.0	51.6
12	syenite STM-1	USGS Certificate of Analysis	27.9	9.7	1.6	2.0	0.1	0.8	6.6	3.6	0.0	52.3
13	NIST glass SRM 610		33.7	1.1				8.6	10.4			53.7
											Average	51.8
											STDEV	1.1

Table S3. Point-by-point correlation between measured elements in the Hanford basaltic clast.

	Na	Mg	Al	Si	K	Ca	V	Fe	Mn	Ni	Cu	Rb	Sr	Zr	Ba	Ce	Pb	Th	U
Na		-0.78	0.77	-0.09	0.28	-0.58	-0.11	-0.27	-0.33	-0.26	-0.09	0.09	0.69	0.07	0.38	0.05	0.01	0.16	-0.05
Mg			-0.85	-0.21	-0.39	0.73	0.1	0.27	0.33	0.26	0.03	-0.15	-0.69	-0.17	-0.44	-0.16	-0.01	-0.31	-0.05
Al				-0.21	0.15	-0.54	-0.07	-0.24	-0.33	-0.25	-0.13	-0.04	0.85	0.02	0.32	-0.01	-0.01	0.08	-0.11
Si					0.43	-0.6	-0.19	-0.16	-0.16	-0.15	0.1	0.38	-0.31	0.2	0.14	0.15	0.01	0.37	0.2
K						-0.52	0	-0.01	-0.08	-0.02	0.19	0.47	0.03	0.34	0.42	0.37	0.14	0.54	0.33
Ca							-0.06	0.02	0.13	0.02	-0.19	-0.33	-0.35	-0.31	-0.49	-0.21	-0.07	-0.43	-0.24
V								0.9	0.58	0.89	0.41	0.01	-0.12	0.27	0.17	0.19	0.08	0.14	0.28
Fe									0.68	0.97	0.58	0.04	-0.25	0.35	0.18	0.26	0.14	0.15	0.4
Mn										0.69	0.53	0.03	-0.25	0.33	0.26	0.47	0.18	0.22	0.6
Ni											0.61	0.05	-0.23	0.36	0.19	0.26	0.1	0.15	0.4
Cu												0.23	-0.07	0.38	0.45	0.35	0.17	0.26	0.63
Rb													-0.09	0.29	0.27	0.29	0.11	0.38	0.32
Sr														-0.06	0.37	-0.01	0	-0.03	-0.08
Zr															0.35	0.42	0.11	0.65	0.46
Ba																0.54	0.18	0.47	0.5
Ce																	0.21	0.62	0.59
Pb																		0.17	0.31
Th																			0.55

Figure S1. Instrumental response (signal intensity) to the liquid internal standards: ^{6}Li, ^{45}Sc, ^{115}In, and ^{209}Bi

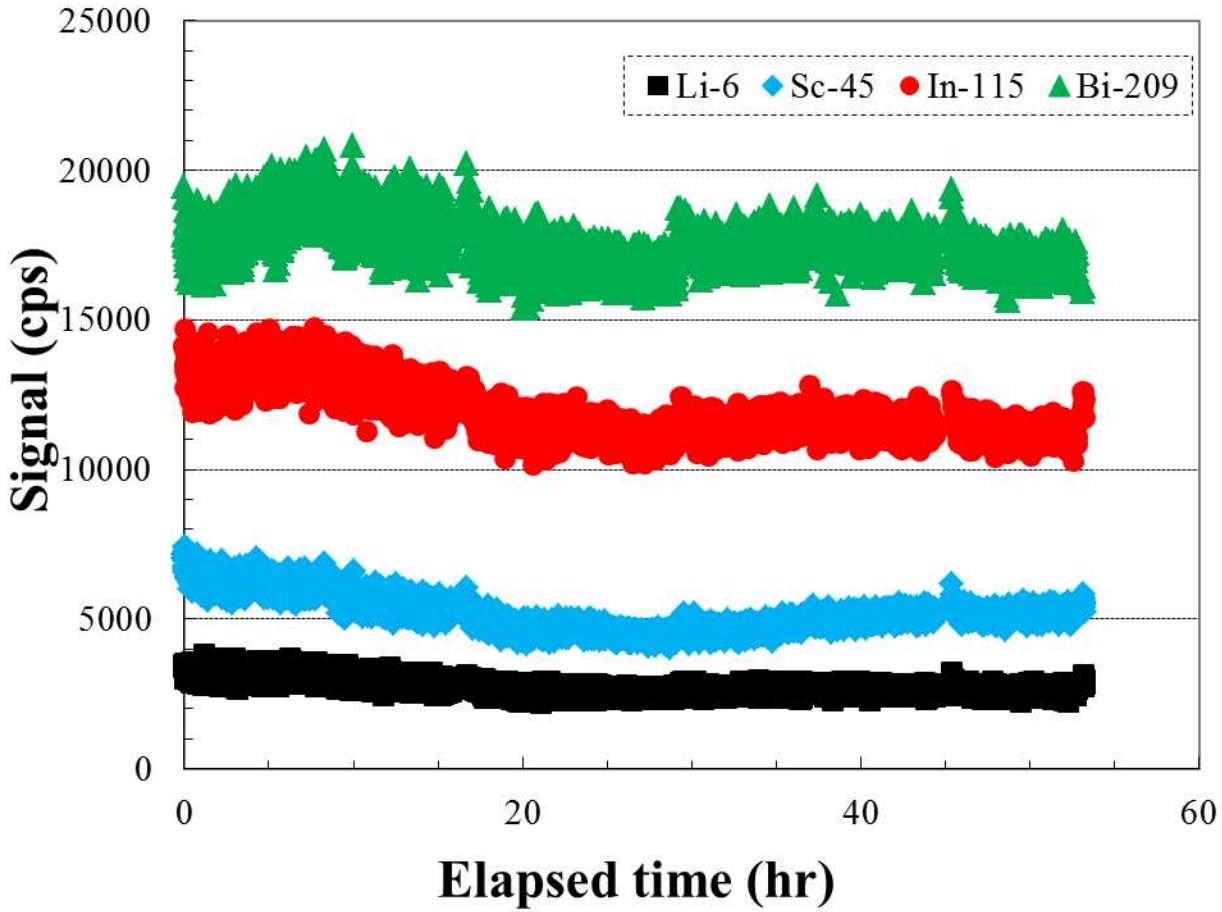

Figure S2. Calculated K^i values for each spot at each depth. K^i values are basically uniform in each layer except for some focused areas. High K^i values correspond to low sampling volume.

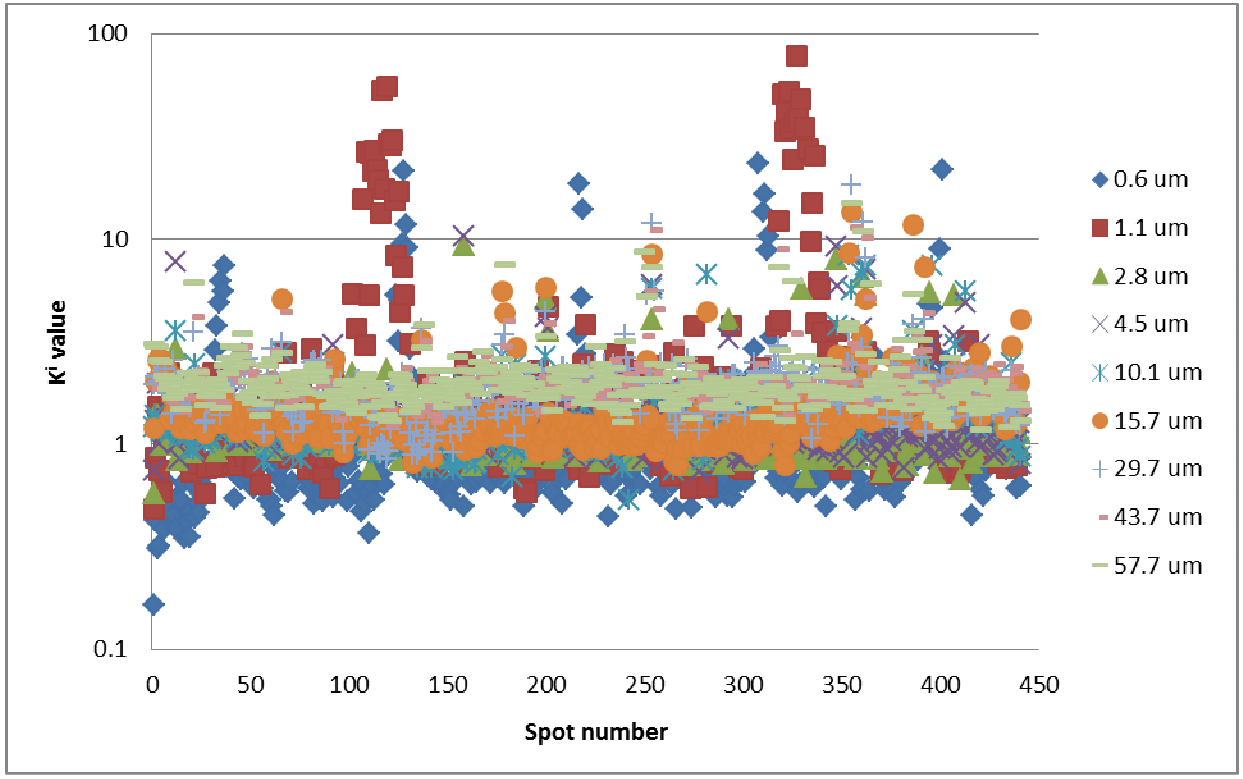

Figure S3. 3-D maps for V, Ni, Mn, Zr, Rb, Th.

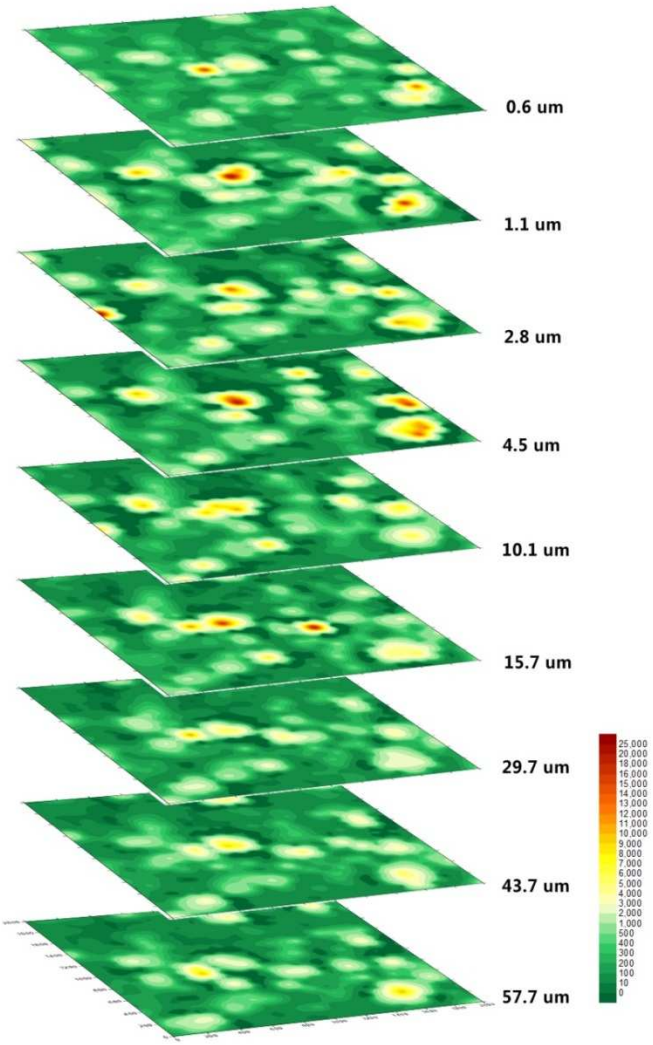
0.6 um
1.1 um
2.8 um
4.5 um
10.1 um
15.7 um
29.7 um
43.7 um
57.7 um
25,000
20,000
18,000
16,000
15,000
14,000
13,000
12,000
11,000
10,000
9,000
8,000
7,000
6,000
5,000
4,000
3,000
2,000
1,000
500
400
300
200
100
10
0

V

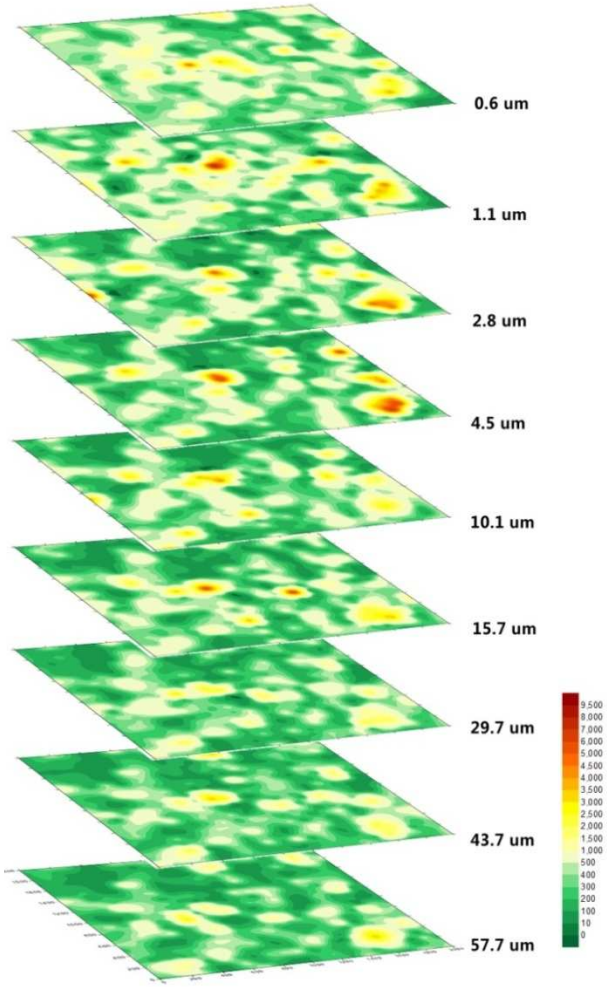
0.6 um
1.1 um
2.8 um
4.5 um
10.1 um
15.7 um
29.7 um
43.7 um
57.7 um
9,500
8,000
7,000
6,000
5,000
4,500
4,000
3,500
3,000
2,500
2,000
1,500
1,000
500
400
300
200
100
10
0

Ni

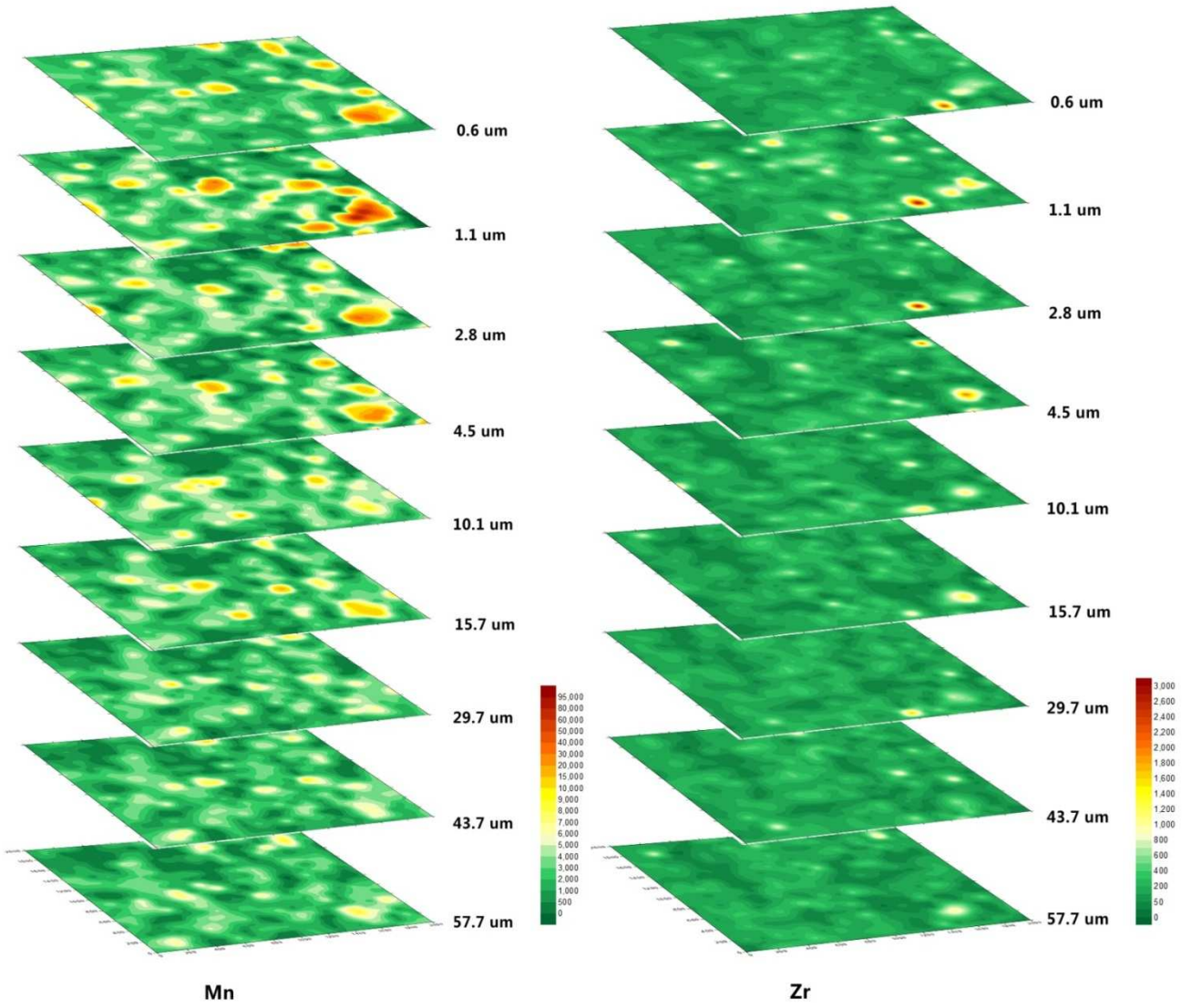
0.6 um
1.1 um
2.8 um
4.5 um
10.1 um
15.7 um
29.7 um
43.7 um
57.7 um
95,000
80,000
60,000
50,000
40,000
30,000
20,000
15,000
10,000
9,000
8,000
7,000
6,000
5,000
4,000
3,000
2,000
1,000
500
0
Mn
0.6 um
1.1 um
2.8 um
4.5 um
10.1 um
15.7 um
29.7 um
43.7 um
57.7 um
3,000
2,600
2,400
2,200
2,000
1,800
1,600
1,400
1,200
1,000
800
600
400
200
50
0
Zr

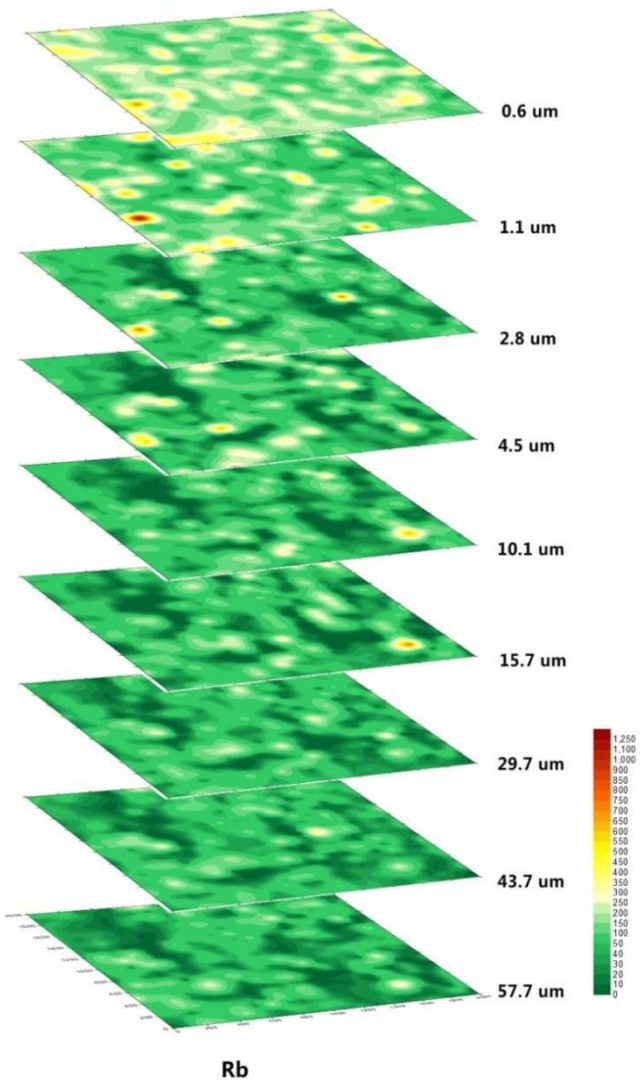
0.6 um
1.1 um
2.8 um
4.5 um
10.1 um
15.7 um
29.7 um
43.7 um
57.7 um
1,250
1,100
1,000
900
850
800
750
700
650
600
550
500
450
400
350
300
250
200
150
100
50
40
30
20
10
0

Rb

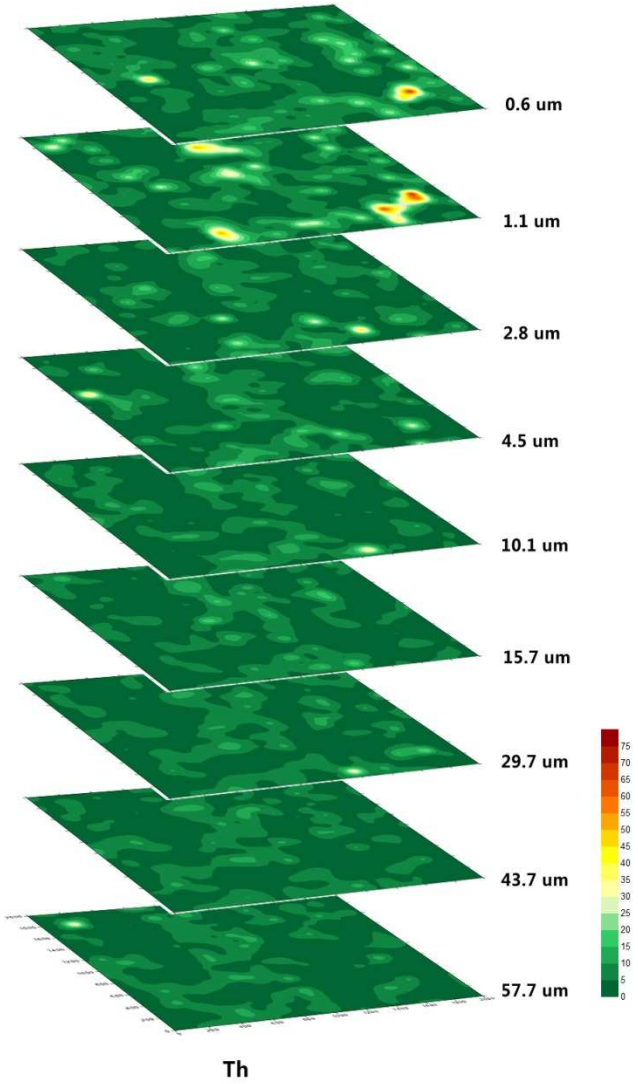
0.6 um
1.1 um
2.8 um
4.5 um
10.1 um
15.7 um
29.7 um
43.7 um
57.7 um
75
70
65
60
55
50
45
40
35
30
25
20
15
10
5
0

Th

Figure S4. Average relative concentrations of intrinsic elements with depth.